WPBB-PR(18) 20701

J.M. Heuser et al.

Radiation stability of long-term annealed bi-phasic advanced ceramic breeder pebbles

Preprint of Paper to be submitted for publication in
Fusion Engineering and Design

This work has been carried out within the framework of the EUROfusion Consortium and has received funding from the Euratom research and training programme 2014-2018 under grant agreement No 633053. The views and opinions expressed herein do not necessarily reflect those of the European Commission.

Radiation stability of long-term annealed bi-phasic advanced ceramic breeder pebbles

Julia M. Heuser[a,*], Arturs Zarins[b,c], Larisa Baumane[b,d], Gunta Kizane[b], Regina Knitter[a]

[a] Karlsruhe Institute of Technology (KIT), Institute for Applied Materials (IAM), 70621 Karlsruhe, Germany

[b] University of Latvia, Institute of Chemical Physics, LV-1004 Riga, Latvia

[c] Daugavpils University, Faculty of Natural Science and Mathematics, Department of Chemistry and Geography, LV-5401 Daugavpils, Latvia

[d] Latvian Institute of Organic Synthesis, LV-1006 Riga, Latvia

*corresponding author: julia.heuser@kit.edu

Abstract

Advanced ceramic breeder pebbles consisting of Li_4SiO_4 and additions of Li_2TiO_3 were tested regarding their long-term thermal and to their radiation stability. As-prepared and long-term annealed pebbles were irradiated with accelerated electrons (up to 6 MGy) to investigate the formation of radiation-induced defects and radiolysis products caused by ionizing radiation. By using Raman spectroscopy the formation of significant amounts of radiolysis products can be excluded. Electron spin resonance spectrometry revealed several paramagnetic radiation-induced defects, such as HC_2 centres (SiO_4^{3-} and TiO_3^{-}), E' centres (SiO_3^{3-} and TiO_3^{3-}), Ti^{3+} centres and peroxide radicals (≡Si-O-O·). Radiation-induced defects forming in the first stage of the radiolysis seem to be more pronounced in long-term annealed samples. Thermally stimulated luminescence showed relatively low temperatures (40–200 °C) for the thermal recovery of the radiation-induced defects by accelerated electrons. Moreover, the main recovery process of defects takes place in the first 8–10 days after the irradiation.

Keywords: fusion technology, advanced ceramic breeder, Li_4SiO_4-Li_2TiO_3, radiation stability, long-term thermal stability

1 Introduction

Different ceramic materials are currently developed for the use as solid breeder materials in future fusion reactors. Lithium orthosilicate (Li_4SiO_4, LOS) and lithium metatitanate (Li_2TiO_3, LMT), applied as pebbles, are considered as ceramic breeder (CB) materials for the European Helium Cooled Pebble Bed (HCPB) blanket concept for Test Blanket Modules (TBM) in ITER and later on for the DEMO reactor. Both materials exhibit good properties to match general requirements of suitable CB pebbles such as resistance to neutron irradiation (fluence of ~10^{22} n·m^{-2} [1]), high temperatures (about 550 °C, peak temperatures of about 900 °C [2, 3], and thermomechanical stresses and they need to provide sufficient tritium for the fusion reaction to reach a tritium breeding ratio TBR ≥ 1.1 [4]. While LOS is favoured due to a higher lithium density, LMT wins over with its higher mechanical strength. Additionally, slightly lower activation properties were reported for LOS, at least when shorter waiting times after shutdown are considered [5, 6], whereas results reported in literature on the tritium release behaviour of these two materials are somewhat contradictory and hardly ever comparable (cf. e.g. [7,

8]). Bi-phasic advanced CB pebbles consisting of LOS and LMT offer an alternative material with the combination of both compositions' advantages and favourable properties. Therefore, at KIT the melt-based KALOS process, which is favourable due to the ease of reprocessing, was designed to produce advanced CB pebbles consisting of LOS with additions of LMT [9–11].

Beside the extensive standard characterisation of this material, knowledge about its long-term thermal as well as its radiation stability is of great concern due to the elevated temperatures and the neutron bombardment the CB material is exposed to in a fusion reactor. Accordingly, a study concerning the long-term thermal stability was performed on three advanced CB compositions [12]. This work moreover combines the thermal with the radiation stability. In a first step, CB pebbles were annealed for up to 128 days at 900 °C, which is expected to be the maximum temperature in a HCPB blanket in DEMO [2, 3], and extensively characterised afterwards. In a second step, as-prepared CB pebbles as well as pebbles with selected annealing durations were irradiated. Because irradiation experiments in a nuclear reactor using neutrons are expensive, time-consuming and require special handling, accelerated electrons were used to introduce radiation-induced defects and radiolysis products (referred to as defects and products in the following text), although nuclear damage in the material is negligible in case of electrons.

2 Material and methods

Advanced CB pebbles, fabricated in the KALOS process, with a nominal composition of 65 mol% LOS and 35 mol% LMT were selected for this study. The as-prepared sample is referred to as KALOS-35 in the following.

With KALOS-35 pebbles a long-term annealing (LTA) experiment and the subsequent material characterisation was performed to investigate the thermal stability of the ceramic pebbles [12]. Therefore, the pebbles were heated in a furnace at 900 °C for up to 128 days. The furnace consists of different tubes, which offers the use of different gas atmospheres at the same time. Each tube is connected to the gas supply (He + 0.1 vol% H_2). One tube features an upstream copper oxide furnace to oxidize the hydrogen of the supplied gas stream to water ($CuO + H_2 \rightarrow Cu + H_2O$). Therefore, the pebbles were annealed in a dry as well as in a moist gas atmosphere under the same temperature programme. Experimental details and methods used for characterisation are described in Heuser et al. [12].

The following three LTA samples with two different LTA durations in days (d) and two different gas atmospheres ("dry" and "H2O") were selected for the irradiation experiment: K-35-LTA-8d-dry, K-35-LTA-128d-dry, and K-35-LTA-128d-H2O. For the irradiation, each sample was encapsulated in a quartz tube in a dry argon atmosphere. Sample KALOS-35 was tempered at 400 °C for 4 h in vacuum to eliminate adsorbed water before the encapsulation. All samples were irradiated with 5 MeV electrons using the linear electron accelerator ELU-4 (Salaspils, Latvia) with a dose rate of 3 MGy/h up to a total absorbed dose of 6 MGy. The temperature was continuously measured with a thermocouple in contact to the quartz tubes during the irradiation time and was in the range of 20–23 °C.

To examine the formed and accumulated defects and products, the irradiated samples were characterised using different techniques and in comparison to the as-prepared sample when reasonable.

Raman spectroscopy was used for phase analysis. Spectra were recorded in the range of 130 to 1100 cm^{-1} with a Renishaw inVia Reflex Raman Microscope using a CCD camera. A 50x ocular was selected of the built-in Leica DM 3000 microscope to focus on the powder sample produced by grinding the pebbles in an agate mortar. With a He-Ne-laser (633 nm, up to 5 mW, 100 % power), a 2400 l/mm grating and an exposure time of 20 s and 5 accumulations, three single points of each sample were measured and the average was used for further data processing in OriginPro 2017 (Academic).

Electron spin resonance (ESR) spectrometry was used to investigate the accumulated paramagnetic defects and products and their development over time after the irradiation. ESR spectra (20 scans) were recorded at room temperature using a Bruker BioSpin GmbH X-band spectrometer (microwave frequency and power: 9.8 GHz and 0.2 mW, modulation amplitude: 5 G, field sweep: 200 and 1000 G, resolution: 1024 pts). The pebbles were analysed in Bruker ER 221TUB/3 CFQ quality sample tubes with an inner diameter of 3 mm. The reference marker Bruker ER 4119HS-2100 (g-factor: 1.9800 ± 0.0005) was used for quantitative measurements. The double integration method was used to determine the total concentration of accumulated paramagnetic defects and products in the irradiated pebbles.

The thermal stability of accumulated defects and products was examined using thermally stimulated luminescence (TSL). The TSL glow curves of pulverized irradiated pebbles were measured with a photomultiplier tube from room temperature up to 400 °C with a heating rate of 2 °C/s. Gaussian functions were applied to the glow curves to unravel the peak positions.

3 Results and discussion

To determine the long-term thermal stability, the ceramic pebbles were characterised before and after the annealing. As described in detail in Heuser et al. [12], the pebbles remain chemically stable, showed only minor changes in their microstructure, the porosities varied slightly over time without any trend and the crush loads decreased about 25 % after one day of annealing and remained at reasonably high values afterwards. Furthermore, no difference in the material properties with regard to the used gas atmosphere was observed.

Raman spectroscopy was used to compare the phase content before and after the irradiation. Structural differences of the LMT phase in the as-prepared sample and the thermally treated samples are revealed in the Raman spectra depicted in figure 1. The spectrum of the as-prepared sample shows broad “amorphous-like” bands (cf. fig. 1, bottom). Broad bands around 810 cm^{-1} with a distinct band observed at 823 cm^{-1} can be assigned to the symmetric stretching vibration v_1 of SiO_4-tetrahedra [13–15]. The overlapping bands in the region of about 200 to 500 cm^{-1} are dominated by vibrations belonging to the LMT phase. More distinct bands can be distinguished in the spectra of the annealed samples. A mixed spectrum of the two phases LOS and LMT was observed, which is similar to Wang

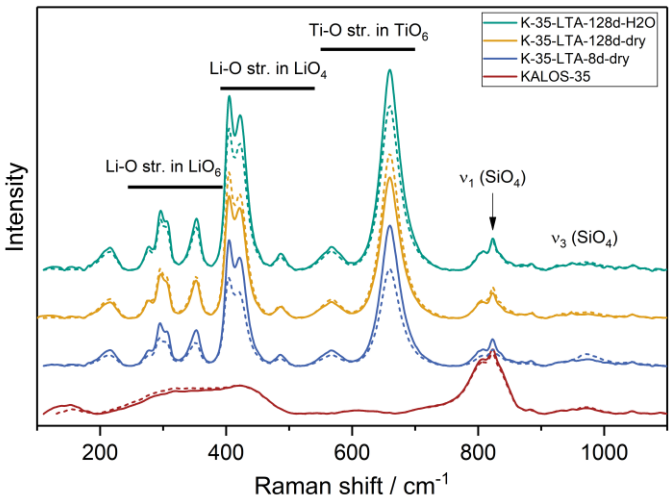

Fig. 1 Raman spectra of all samples before (solid lines) and after the irradiation (dashed lines).

et al. [15]. Although the LOS content is higher, the spectrum predominantly reveals bands that can be assigned to the LMT phase (cf. a Raman spectrum of pure LMT [16]). Ti-O as well as Li-O stretching vibrations in the different polyhedra generate bands in the following wavenumber regions: Bands in the region of 250 to 400 cm^{-1} can be assigned to a Li-O stretching in the LiO_6 octahedra. Within 400 to 550 cm^{-1}, bands belong to the Li-O stretching in the LiO_4 tetrahedra and a Ti-O stretching in the TiO_6 octahedra is observed by the appearance of bands within 550 to 700 cm^{-1} [15–17]. Like in the spectrum of KALOS-35, the main band of the v_1 of SiO_4 is located at 823 cm^{-1} for all LTA samples. Antisymmetric stretching vibrations v_3 occur at higher wavenumbers with no distinct bands.

After irradiation no major changes such as additional bands or increased band widths in the Raman spectra of the pebbles were detected (see figs. 1 dashed lines) and thus these results will not further be discussed. Yet, due to the relatively small absorbed dose and low irradiation temperature, significant changes were not expected [18, 19].

ESR spectra measured after the electron irradiation reveal several first derivative signals, that were attributed to different groups of paramagnetic defects and products. ESR signals recorded 2 h after the irradiation are shown in figure 2 and are comparable to spectra in previous studies on advanced CB pebbles [20–22].

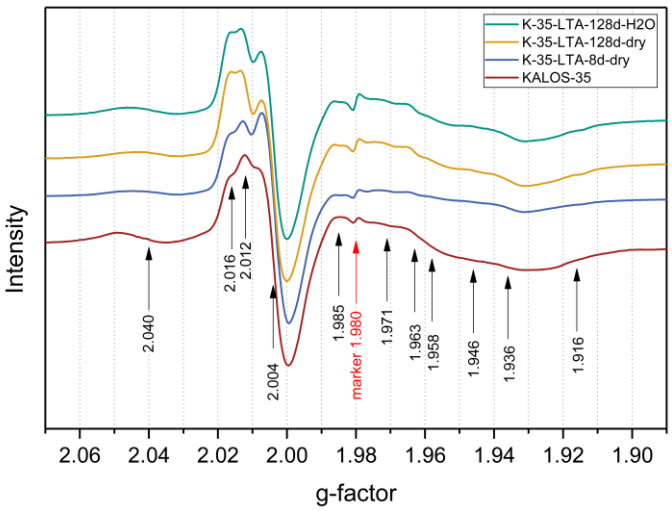

Fig. 2 Normalised ESR spectra of all samples 2 h after the irradiation and the observed signals.

The observed ESR signals with g-factors of 2.016 ± 0.001 and 2.012 ± 0.001 can assigned to HC_2 centres (SiO_4^{3-} and TiO_3^{-}), and 2.004 ± 0.001 to E' centres (SiO_3^{3-} and TiO_3^{3-}) [23, 24], whereas g-factors of 2.040 ± 0.001 might be assigned to peroxide radicals (≡Si-O-O·) [21, 25]. The group of the ESR signals with g-factors between 1.971 and 1.936 is ascribed to "Ti^{3+} ion trapped-electron centres" [26], where an electron is captured by a Ti^{4+} ion and is reduced to Ti^{3+}, referred to as Ti^{3+} centres in the following. In comparison to Zarins et al. [20, 22], additional ESR signals with g-factors 1.916 and 1.985 were detected in the present study, which were more pronounced in the LTA samples. Because the g-factors are close to the before mentioned region, these signals might also be caused by Ti^{3+} centres. As these additional signals are more pronounced in the LTA samples, they probably were not detectable in previous studies [20–22]. As the signals for Ti^{3+} centres are in general lower for LTA samples, the detection of additional signals might be an effect of increased resolution. F^+ centres cannot completely be excluded due to a lack of reference data and because the broad signal of low intensity with an available g-factor of 2.003 in a study about Li_2O [27] might be overlapped by the observed signal of E' centres. A narrow signal for colloidal lithium particles (g-factor 2.0023–2.0025 [19, 27, 28]) was not detected.

Table 1 summarises the possible paramagnetic defects and products and their appropriate g-factors. Moreover, the spectra reveal differences regarding the annealing conditions of several samples, esp. in the g-factor region of 2.00 to 2.02 (cf. fig. 2). While differences occur with regard to the time of annealing, the gas atmosphere seems to have no influence on the paramagnetic defects and products detected with ESR. In LTA samples the HC_2 and E' centres seem to be more pronounced, while peroxide radicals and Ti^{3+} centres seem to have a lower contribution than in unannealed samples. This indicates that defects forming in the first stage of radiolysis [18, 19, 25] are dominant for the LTA pebbles, whereas defects forming in the second stage of radiolysis and the formation of Ti^{3+} centres seems to be less likely.

Table 1 ESR signals and the possible radiation-induced paramagnetic defects and/or radiolysis products. Detected signals marked with an asterisk are more pronounced in LTA samples.

g-factor	Possible radiation-induced defects or radiolysis products	Detection
2.040 ± 0.001	Peroxide radical (≡Si-O-O·)	✓
2.016 ± 0.001	HC_2 centre (SiO_4^{3-}, TiO_3^-)	✓
2.012 ± 0.001	HC_2 centre (SiO_4^{3-}, TiO_3^-)	✓
2.004 ± 0.001	E' centre (SiO_3^{3-}, TiO_3^{3-})	✓
2.003	F^+ centre (value for Li_2O)	?
2.0023–2.0025	Colloidal lithium (Li_n) (value for Li_2O)	-
1.985 ± 0.010	Not assigned, possibly Ti^{3+} centre	✓*
1.971 ± 0.010	Ti^{3+} centre	✓
1.963 ± 0.010	Ti^{3+} centre	✓
1.958 ± 0.010	Ti^{3+} centre	✓
1.946 ± 0.010	Ti^{3+} centre	✓
1.936 ± 0:010	Ti^{3+} centre	✓
1.916 ± 0.010	Not assigned, possibly Ti^{3+} centre	✓*

To investigate the development and recovery of the paramagnetic defects and products after the irradiation, further ESR spectra were recorded over a time up to 1152 h after the irradiation. Figure 3 shows normalised spectra for all measuring times of each sample. Arrows indicate the trend of ESR signals over time. For the unannnealed sample KALOS-35, a decrease of peroxide radicals, E' and Ti^{3+} centres are observed, while there is a slight increase in the region of HC_2 centres. K-35-LTA-8d-dry exhibits the lowest changes after irradiation and almost only an increase in the region of the HC_2 centres is observed. The two LTA samples annealed for 128 d reveal a comparable behaviour of defects and products. In K-35-LTA-128d-dry and -H2O there is rather no development in the type of defects and products over time after the irradiation, so that only slight changes in the normalised spectra are detected. With a known defect concentration of the marker, it was possible to determine the total concentration of accumulated paramagnetic defects and products using the double integration method. The unannealed sample KALOS-35 has the highest concentration, followed by K-35-LTA-8d-dry and the concentrations of unpaired spins for the samples annealed for 128 d is the lowest and alike for both atmospheres during LTA. This can be explained by a higher ordered structure with a lower amount of initial intrinsic point defects. The concentration of paramagnetic defects decreases slightly with time after the irradiation within the first ~200 h and stays more or less constant afterwards within the same order of magnitude (see fig. 4).

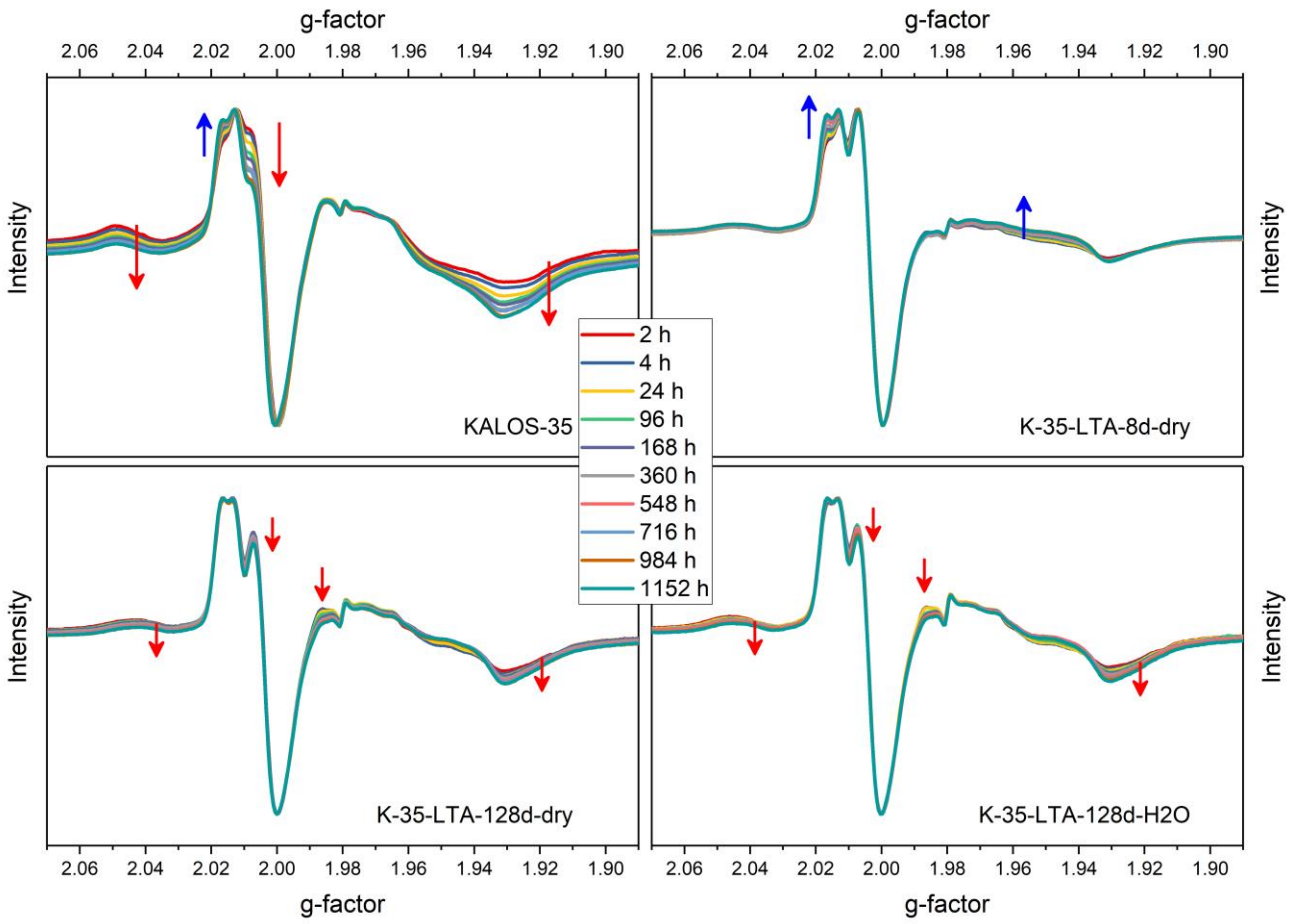

Fig. 3 Normalised ESR spectra for all samples for different durations after the irradiation.

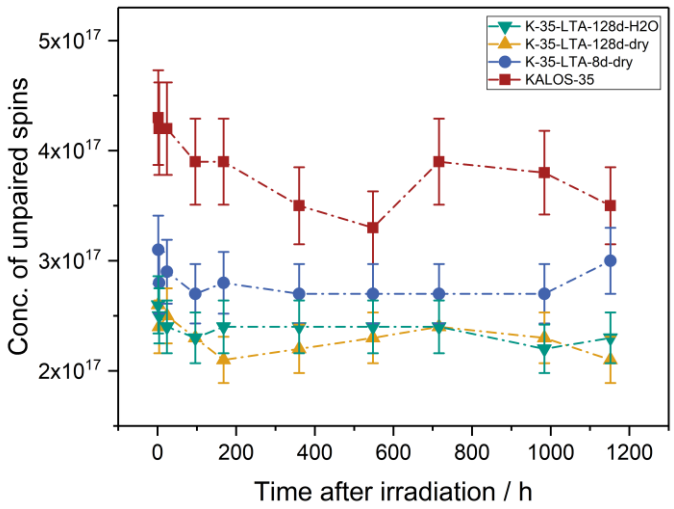

Fig. 4 Total concentration of unpaired spins for all samples over time after the irradiation.

In addition to ESR measurements, TSL glow emission curves were measured to get information about the thermally stimulated recombination of defects and products. Furthermore, TSL glow curves were re-measured in different time intervals from 24 to 1200 h after the irradiation to investigate the development of defects comparable to the ESR analysis.

Figure 5 shows the measured glow curves for all samples recorded 24 h after the irradiation with accelerated electrons. After the deconvolution of the curves, peak maxima at about 80, 100, 140–180 and for some curves at about 290 °C were obtained. After about 240 h a peak at ~60 °C is recognized. A new appearance of a peak indicating a new defect would be unlikely. Therefore, it is reasonable to assume that it becomes more pronounced due to a decrease of the other peaks, which would go along with a higher thermal stability. The area of glow curves was determined for each sample up to 1200 h after the irradiation to deduce information about the development of defect concentrations over time. The development of the TSL signals' area is depicted in figure 6.

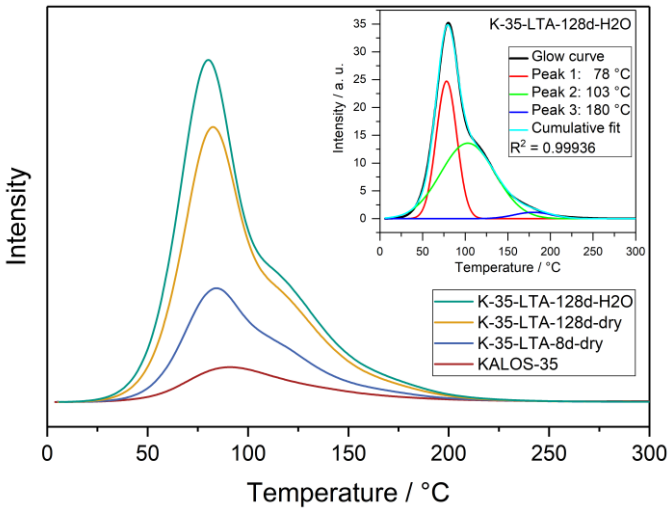

Fig. 5 TSL glow curves of all samples 24 h after the irradiation. The small figure shows the deconvolution of the glow curve exemplary for sample K-35-LTA-128d-H2O.

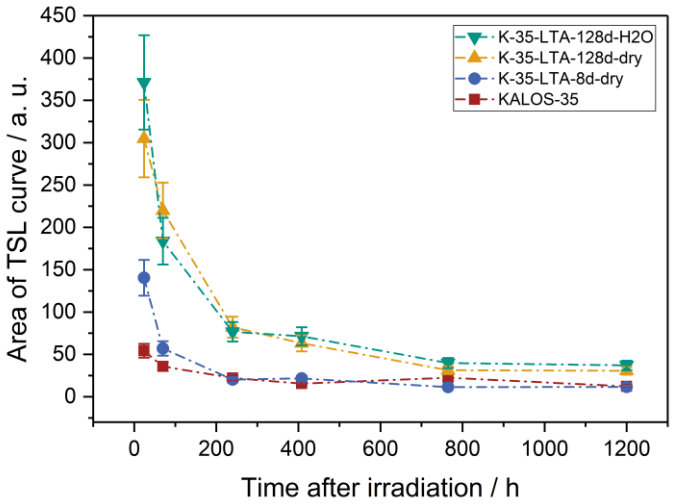

Fig. 6 Development of the area of the integrated TSL curves in the different irradiated samples over time after the irradiation.

It can be seen that the longer the annealing duration of the sample independently of the gas atmosphere, the higher the defect concentration. This seems to be a contrast to the ESR, however the detection of the two techniques are not comparable and therefore, not the same defects and products are analysed. Whereas unpaired spins that were generated during ionising radiation are detected with ESR, the TSL technique recognises defects that recover under thermal stimulation. A

significant decrease of defects can be observed over time. The recovery process mainly takes place within the first ten days after the irradiation. This recovery time is comparable with that of the ESR measured defects. Furthermore, the temperatures of the peak maxima change more or less over time. A clear trend was observed for the main peak, where the peak temperature increases with time (see fig. 7). This indicates that the remaining defects need higher energies for their recovery the longer the time after the irradiation. This is probably because over time the lower-energy defects have recovered and the number of defects that are bonded tighter in the material have relatively increased and therefore, higher energies are needed for their recovery. The observed peak maxima have generally lower peak temperatures compared to previous studies [21, 22] which is most likely an effect of the lower irradiation temperature used in the present study. Therefore, it can be assumed that on the one hand there are less generated defects, which is confirmed by the ESR analysis, and on the other hand less energy is needed to recover them. The temperature for the recovery process of the main signal was slightly lower the longer the LTA time of the samples.

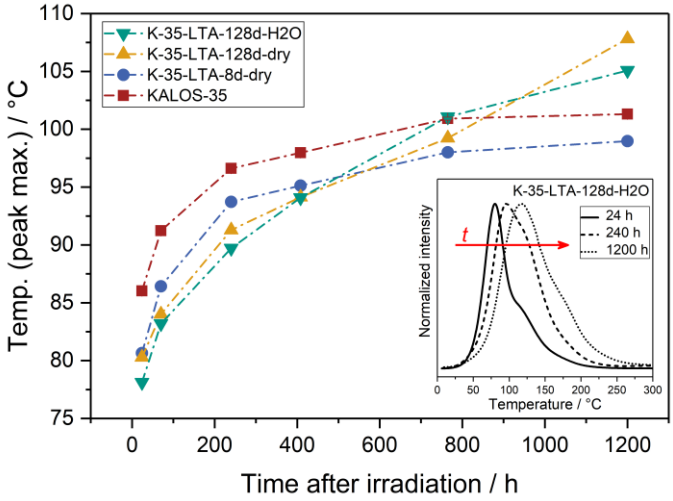

Fig. 7 Development of peak temperature of the main peak in TSL glow curves of all irradiated samples over time after the irradiation. The small figure shows the shift to higher temperatures of selected normalised TSL glow curves over time (*t*) exemplary for sample K-35-LTA-128d-H2O.

4 Conclusions

As-prepared and selected long-term annealed (900 °C up to 128 d) advanced CB pebbles (LOS incl. ~35 mol% LMT) were irradiated in dry argon atmosphere with accelerated 5 MeV electrons up to 6 MGy at room temperature (dose rate 3 MGy/h). The radiation-induced decomposition or formation of new phases were not detected by Raman spectroscopy. ESR spectrometry shows the formation and accumulation of various paramagnetic radiation-induced defects, such as peroxide radicals, Ti^{3+}, HC_2 and E' centres. HC_2 and E' centres, which are formed in the first stage of radiolysis, seem to be more pronounced in LTA samples, whereas peroxide radicals and Ti^{3+} centres seem to be less pronounced. For all samples the characteristic ESR signals of small colloidal lithium particles and F^+ centres were not detected. The longer the samples were annealed, the lower the concentration of accumulated paramagnetic radiation-induced defects and radiolysis products. In general, the concentration of paramagnetic defects only slightly decreases over time after the irradiation. However, additional TSL analyses reveal more radiation-induced defects in LTA samples. After the irradiation

a rapid recovery of the defects is observed. Accumulated radiation-induced defects and radiolysis products recombine in a temperature region of about 40 to 200 °C. Moreover, the duration of the LTA leads to a slight decrease in the temperatures for the recombination of defects. In general, no influence of the gas atmosphere during annealing on the radiation behaviour was observed.
This study combined experiments on the long-term thermal and radiation stability for the first time. The tested advanced CB pebbles show a high thermal stability over time and a good recovery behaviour. Furthermore, a LTA in dry as well as in moist atmosphere does not deteriorate their radiation stability and the recovery of defects seems to be slightly enhanced. Further experiments on neutron irradiated samples are necessary to derive statements on the comparison of using accelerated electrons for the investigation of radiation-induced defects and radiolysis products in CB materials.

Acknowledgements

The authors greatly acknowledge the experimental and technical support of Thomas Bergfeldt, Benjamin Fretz, Ulrike Kaufmann, Oliver Leys, Christina Odemer, Margarete Offermann, Rafael Wramba (KIT), Liga Avotina (Univ. of Latvia), and Aleksandrs Petjukevics (Daugavpils Univ.). Furthermore, Julia M. Heuser acknowledges the financial support of the EUROfusion Engineering Grant EEG-2016/01. This work has been carried out within the framework of the EUROfusion Consortium and has received funding from the Euratom research and training programme 2014-2018 and 2019-2020 under grant agreement No 633053. The views and opinions expressed herein do not necessarily reflect those of the European Commission.

References

[1] U. Fischer, C. Bachmann, I. Palermo, P. Pereslavtsev, R. Villari, “Neutronics requirements for a DEMO fusion power plant”, Fusion Eng. Des. 98–99 (2015) 2134–2137.

[2] L.V. Boccaccini, G. Aiello, J. Aubert, C. Bachmann, T. Barrett, A. Del Nevo, D. Demange, L. Forest, F. Hernández, P. Norajitra, G. Porempovic, D. Rapisarda, P. Sardain, M. Utili, L. Vala, “Objectives and status of EUROfusion DEMO blanket studies”, Fusion Eng. Des. 109 (2016) 1199–1206.

[3] F. Hernández, P. Pereslavtsev, Q. Kang, P. Norajitra, B. Kiss, G. Nádasi, O. Bitz, “A new HCPB breeding blanket for the EU DEMO: Evolution, rationale and preliminary performances”, Fusion Eng. Des. 124 (2017) 882–886.

[4] P. Pereslavtsev, C. Bachmann, U. Fischer, “Neutronic analyses of design issues affecting the tritium breeding performance in different DEMO blanket concepts“, Fusion Eng. Des. 109–111 (2016) 1207–1211.

[5] M. Chen, Q. Huang, S.L. Zheng, “Activation analysis of tritium breeder materials in the FDS-II fusion power reactor”, Fusion Eng. Des. 82 (2007) 2641–2646.

[6] K. Mukai, P. Pereslavtsev, U. Fischer, R. Knitter, “Activation calculations for multiple recycling of breeder ceramics by melt processing”, Fusion Eng. Des. 100 (2015) 565–570.

[7] C.E. Johnson, “Tritium behavior in lithium ceramics”, J. Nucl. Mater. 270 (1999) 212–220.

[8] T. Kinjyo, M. Nishikawa, N. Yamashita, T. Koyama, T. Tanifuji, M. Enoeda, “Chemical form of released tritium from solid breeder materials under the various purge gas conditions”, Fusion Eng. Des. 82 (2007) 2147–2151.

[9] M.H.H. Kolb, R. Knitter, U. Kaufmann, D. Mundt, “Enhanced fabrication process for lithium orthosilicate pebbles as breeding material”, Fusion Eng. Des. 86 (2011) 2148–2151.

[10] R. Knitter, M.H.H. Kolb, U. Kaufmann, A.A. Goraieb, “Fabrication of modified lithium orthosilicate pebbles by addition of titania”, J. Nucl. Mater. 442 (2013) S433–S436.

[11] O. Leys, T. Bergfeldt, M.H.H. Kolb, R. Knitter, A. Goraieb, “The reprocessing of advanced mixed lithium orthosilicate/metatitanate tritium breeder pebbles”, Fusion Eng. Des. 107 (2016) 70–74.

[12] J.M. Heuser, M.H.H. Kolb, T. Bergfeldt, R. Knitter, “Long-term thermal stability of two-phased lithium orthosilicate/metatitanate ceramics”, J. Nucl. Mater. 507 (2018) 396–402.

[13] K. Nakamoto, “Infrared and Raman spectra of inorganic and coordination compounds”, Handbook of Vibrational Spectroscopy, John Wiley & Sons, Ltd. (2006).

[14] V.V. Fomichev and E.V. Proskuryakova, “Vibrational spectra and energy characteristics of the superionics Li_4SiO_4 and Li_4GeO_4”, J. Solid State Chem. 134 (1997) 232–237.

[15] Y. Wang, Q. Zhou, L. Xue, H. Li, Y. Yan, “Synthesis of the biphasic mixture of Li_2TiO_3-Li_4SiO_4 and its irradiation performance”, J. Eur. Ceram. Soc. 36 (2016) 4107–4113.

[16] T. Nakazawa, A. Naito, T. Aruga, V. Grismanovs, Y. Chimi, A. Iwase, S. Jitsukawa, “High energy heavy ion induced structural disorder in Li_2TiO_3”, J. Nucl. Mater. 367-370, Part B (2007) 1398–1403.

[17] Ch.-L. Yu, D.-P. Gao, K. Yanagisawa, “Vacancy and substitution defects of β-Li_2TiO_3 prepared by hydrothermal method”, Chem. Lett. 43 (2014) 369–370.

[18] J.E. Tiliks, G.K. Kizane, A.A. Supe, A.A. Abramenkovs, J.J. Tiliks, V.G. Vasiljev, “Formation and properties of radiation-induced defects and radiolysis products in lithium orthosilicate”, Fusion Eng. Des. 17 (1991) 17–20.

[19] J. Tiliks, G. Kizane, A. Vitins, G. Vitins, J. Meistars, “Physicochemical processes in blanket ceramic materials”, Fusion Eng. Des. 69 (2003) 519–522.

[20] A. Zarins, O. Valtenbergs, G. Kizane, A. Supe, S. Tamulevicius, M. Andrulevicius, E. Pajuste, L. Baumane, O. Leys, M.H.H. Kolb, R. Knitter, “Characterisation and radiolysis of modified lithium orthosilicate pebbles with noble metal impurities”, Fusion Eng. Des. 124 (2017) 934–939.

[21] A. Zarins, O. Valtenbergs, G. Kizane, A. Supe, R. Knitter, M.H.H. Kolb, O. Leys, L. Baumane, D. Conka, “Formation and accumulation of radiation-induced defects and radiolysis products in modified lithium orthosilicate pebbles with additions of titanium dioxide”, J. Nucl. Mater. 470 (2016) 187–196.

[22] A. Zarins, O. Leys, G. Kizane, A. Supe, L. Baumane, M. Gonzalez, V. Correcher, C. Boronat, A. Zolotarjovs, R. Knitter, “Behaviour of advanced tritium breeder pebbles under simultaneous action of accelerated electrons and high temperature”, Fusion Eng. Des. 121 (2017) 167–173.

[23] V. Grismanovs, T. Kumada, T. Tanifuji, T. Nakazawa, “ESR spectroscopy of γ-irradiated Li_2TiO_3 ceramics”, Radiat. Phys. Chem. 58 (2000) 113–117.

[24] Y. Nishikawa, M. Oyaidzu, A. Yoshikawa, K. Munakata, M. Okada, M. Nishikawa, K. Okuno, “Correlation between tritium release and thermal annealing of irradiation damage in neutron-irradiated Li_2SiO_3“, J. Nucl. Mater. 367-370 (2007) 1371–1376.

[25] A. Abramenkovs, J. Tiliks, G. Kizane, V. Grishmanovs, A. Supe, “Basic study of influence of radiation defects on tritium release processes from lithium silicates”, J. Nucl. Mater. 248 (1997) 116–120.

[26] P. Lombard, N. Ollier, B. Boizot, “EPR study of Ti^{3+} ions formed under beta irradiation in silicate glasses”, J. Non-Cryst. Solids 357 (2011) 1685–1689.

[27] P. Vajda and F. Beuneu, “Electron radiation damage and Li-colloid creation in Li2O”, Phys. Rev. B 53 (1996) 5335–5340.

[28] F. Beuneu, P. Vajda, G. Jaskierowicz, M. Lafleurielle, “Formation of two kinds of nonspherical lithium colloids in electron-irradiated Li_2O single crystals”, Phys. Rev. B 55 (1997) 11263–11269.